

Subharmonic nuclear spin echo in domain walls

L. L. Buishvili, G. I. Mamniashvili, and M. G. Menabde

Institute of Physics, Academy of Sciences of the Georgian SSR, Tbilisi

(Submitted 31 March 1986)

Zh. Eksp. Teor. Fiz. **91**, 1755–1761 (November 1986)

A subharmonic spin echo of the nuclei located in domain walls of manganese ferrite was observed experimentally at $T = 77$ K. This echo was explained by the Hahn mechanism. The proposed theoretical model agrees qualitatively with the available experimental data.

The effects of subharmonic pulses on the nuclear spin system have been observed so far for lithium ferrite, thin cobalt films, and easy-plane antiferromagnet FeBO_3 . Signals of the nuclear spin echo due to the ^{57}Fe nuclei in polycrystalline samples of lithium ferrite and thin cobalt films subjected to subharmonic excitation in zero external field at $T = 300$ K were observed by Dudkin *et al.*¹ The mechanism of the excitation of the echo signals was not identified in Ref. 1. In the case of the easy-plane antiferromagnet FeBO_3 with weak ferromagnetism at $T = 77$ K the echo signals did not appear when subharmonic pulses were generated. However, these pulses did influence the conventional echo.

This influence was attributed to the excitation of magnetoelastic oscillations at the resonance frequency due to nonlinear effects.²

Magnetically ordered crystals are, in principle, capable of exhibiting one further form of excitation of the nuclear spin system by a nonresonance interaction, namely the nonlinear properties of domain walls may give rise to a signal due to the nuclei located in these walls when the excitation is in the form of subharmonic pulses. A study of this excitation is reported below.

MEASUREMENT METHOD

All the measurements were carried out on a polycrystalline sample of manganese ferrite MnFe_2O_4 at liquid nitrogen temperature. This sample was a rectangular slab with typical dimensions of ≈ 3 mm. A signal was generated using a pulse NMR spectrometer operating in the frequency range 500–1300 MHz; the block diagram of this spectrometer and its parameters were similar to those reported in Refs. 3 and 4. Generators produced pulses at the resonance frequency f and also at subharmonic frequencies $f/2$ and $f/3$. These rf pulses were applied by the generators to a single-turn coil surrounding the sample. The echo signal was received by a second coil and applied to a superheterodyne detector. From this detector the signal was sent to an oscilloscope, the screen of which was used for displaying the signal as a function of time. The second input of the oscilloscope received signals from wavemeters used to measure the resonance frequency. An electronic counting frequency meter of the Ch3-45 type was used to measure the frequencies $f/2$ and $f/3$. The delay t_{12} between the pulses was set by G5-35 precision decade pulse generators. The signal echo amplitude was determined from the oscilloscope screen. A static magnetic field was created by the electromagnet from the rf spectrometer and was measured using a Hall sensor.

EXPERIMENTAL RESULTS

We investigated manganese ferrite MnFe_2O_4 in which the large magnetic moment of the ^{55}Mn nuclei ($\mu = 3.47 \mu_n$), 100% abundance of the investigated ^{55}Mn isotope, and the weak anisotropy ensured a strong NMR signal. This is why manganese ferrite has become an object of intensive investigations by the magnetic spin echo and other NMR methods. The results of these investigations have been the subject of a critical analysis and refinement in Ref. 5. The spectrum of the nuclei located in domain walls of polycrystalline MnFe_2O_4 at $T = 1.7$ K, exhibiting the dynamic frequency shift effect, is also given in Ref. 5. The dynamic frequency shift is due to coupled oscillations of the nuclear magnetization and of domain walls due to the proximity of their resonance frequencies.^{5,6} Moreover, the spectrum of the nuclei located in domain walls but not exhibiting the dynamic frequency shift is reported in Ref. 7. The shift of the nuclei in domain walls is observed only at low temperatures ($T = 1.7$ – 3.0 K). At higher temperatures no properties of the echo other than the Hahn parameters⁸ have been observed for MnFe_2O_4 . This was why we selected the temperature to be $T = 77$ K. We observed the spin echo signals of the ^{55}Mn nuclei when the spin system was excited at the second and third subharmonics due to application of excitation pulses in the following combinations $(f/2, f)$, $(f, f/2)$, $(f/2, f/2)$, $(f/3, f)$. Irrespective of the excitation frequency the echo was observed at the frequency f . The subharmonic echo spectrum was practically identical with the spin echo spectrum of the ^{55}Mn nuclei located in domain walls. The strongest echo signals was observed for the excitation pulse combinations $(f/2, f)$ and $(f/2, f/2)$. Figure 1b shows the echo signal excited by two pulses at the second subharmonic. This investigation showed that, in some range of frequencies, the dependence of the echo intensity on the rf pulse power under resonance excitation conditions exhibits additional maxima at low rf pulse powers.

The properties of the nuclear spin echo near the secondary maximum were found to be quite different from those at high rf pulse powers. The transverse relaxation times in these two cases were $T_2 = 3.6 \pm 0.3 \mu\text{s}$ and $T_2 > 5 \mu\text{s}$, respectively, and in the former case the relaxation time was practically constant over the spectrum, whereas in the latter case it rose at the edges of the spectrum. The echo intensity at low rf pulse powers decreased considerably in magnetic fields $H > 2$ – 3 kOe and the optimal power was practically independent of the external magnetic field. An analysis of these re-

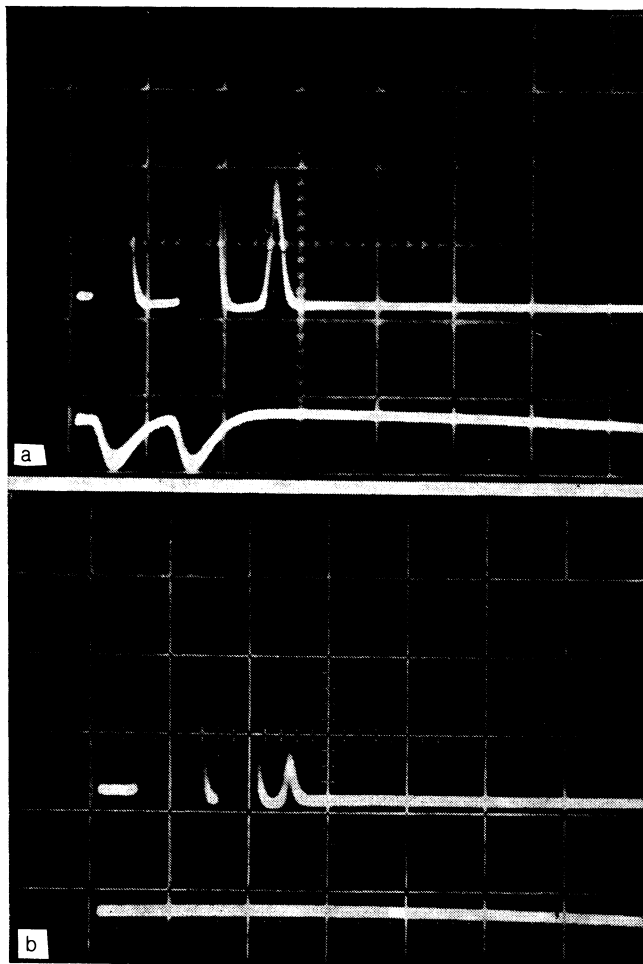


FIG. 1. Echo signals of the ^{55}Mn nuclei in MnFe_2O_4 under resonance excitation conditions (a) and on excitation with two pulses at the second subharmonic (b). The lower trace is the signal from a wavemeter tuned to the resonance frequency $f = 582.2$ MHz. Delay between pulses $t_{12} = 7 \mu\text{s}$, $\tau_1 = \tau_2 = 1.1 \mu\text{s}$ (a), $\tau_1 + 4.3 \mu\text{s}$, $\tau_2 = 1.1 \mu\text{s}$ (b). Horizontal scale $5 \mu\text{s}/\text{cm}$.

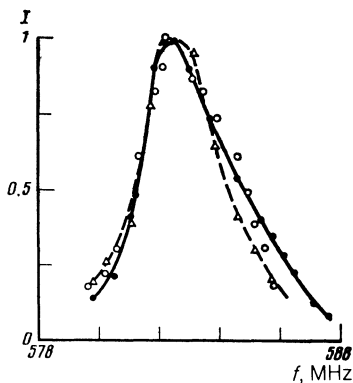


FIG. 2. Spectra of the echo signals of the ^{55}Mn nuclei in: (●) spectrum of the echo from the nuclei located in domain walls under resonance excitation conditions; (○) spectrum obtained on excitation with the first pulse at the second subharmonic and with the second resonance pulse; (Δ) spectrum obtained on application of two pulses at the second subharmonic. The conditions are optimal for each of these cases. The echo intensities are normalized.

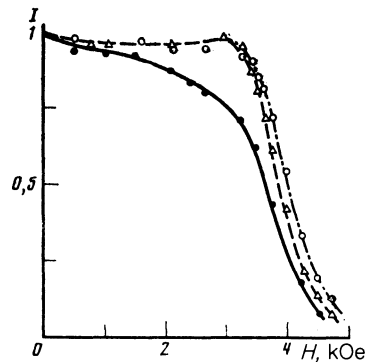


FIG. 3. Dependences of the intensities of the echo signals on the external magnetic field H : (●) nuclei located in domain walls excited by resonance pulses; (○) excited by a pulse at the second subharmonic and by a second resonance pulse; (Δ) excited by two pulses at the second subharmonic.

sults indicated that the ^{55}Mn nuclei investigated by the observation of the echo signals in the range of low rf pulse powers were located in domain walls. On the other hand, at high rf pulse powers we observed the spin echo of the nuclei in the domains themselves. The spectrum of the spin echo of the nuclei in domain walls and the spectra of the echo signals excited at the second harmonic and in the presence of the rf pulses in the combination $(f/2, f)$ are plotted in Fig. 2. As in the case of the echo signals excited at NMR frequency, the echo signals excited at the subharmonic frequencies disappeared on magnetization of the sample when the domain walls disappeared (this happened for $4\pi M/3 = 2.2$ kOe for MnFe_2O_4 at $T = 77$ K, see Fig. 3).

The transverse relaxation time for the investigated echo signals observed at the subharmonics was found to be constant over the spectrum and equal to $T_2 = 2.6 \pm 0.2 \mu\text{s}$. At $f = 582.2$ MHz for the $(f, f/2, f)$ sequence of rf pulses the decay time constant of the stimulated echo was $T_1 \approx 10 \mu\text{s}$, which was close to the value for the ordinary stimulated echo at the same frequency. Special investigations carried out at different NMR frequencies using different rf pulse durations and powers established that the properties of the spin echo excited at the subharmonic frequency did not differ from the properties of the Hahn echo.⁸ The maximum intensity of the echo for the $(f/2, f/2)$ sequence was approximately an order of magnitude less than the intensity of the ordinary echo signal. However, one should point out that in our case the powers of the subharmonic rf pulses did not reach the optimal value. At the optimal power one could expect, as in Ref. 1, the intensities of the echo signals excited at the subharmonics to be of the order of the intensities of the echo signals excited by the resonance frequency pulses.

A qualitative idea of the relationships between the optimal rf pulse powers for these signals was obtained by determining the dependence of the ordinary echo and that excited by the $(f/2, f)$ sequence on the duration τ_1 of the first pulse. The two cases were characterized by practically the same power of the second resonance rf pulse optimal for the observation of the echo signals. The measurements indicated that the echo signal excited by the sequence $(f/2, f)$ of the same intensity as that of the ordinary echo at low values of τ_1

required at least an order of magnitude higher power of the rf pulses.

These experimental results indicated that the echo signals excited at the subharmonics in MnFe_2O_4 at $T = 77$ K were due to the ^{55}Mn nuclei located in the domain walls and they were formed as a result of the Hahn mechanism.

THEORETICAL MODEL

We shall consider the simplest case of a 180° domain wall, which represents a transition layer between two planar domains, in one of which the spins are parallel and in the other antiparallel to the z axis. The angle θ_j , which determines the equilibrium direction of the spin in the xz plane, varies in accordance with the law⁹

$$\sin \theta_j = 1/\text{ch} \left(\frac{y_j}{\delta} \right),$$

where δ is the domain wall width.

The Hamiltonian of such a domain wall can be represented in the form of a sum of the energies of magnons of two types: specific intradomain magnons and magnons which are a modification of ordinary spin waves in a single-domain ferromagnet.^{9,10} We shall consider only the first type of these elementary excitations. In this case the Hamiltonian of the electron-nuclear system representing a domain wall with local coordinates in which the z axis coincides with the equilibrium magnetization can be represented in the form^{9,10}

$$\begin{aligned} \mathcal{H} = & \sum_{\mathbf{k}} \varepsilon_{\mathbf{k}} a_{\mathbf{k}}^+ a_{\mathbf{k}} + \sum_j A S_j I_j \\ & + \sum_j 2\omega_1 (S_j^z \cos(\theta_j + \varphi) + S_j^x \sin(\theta_j + \varphi)) \cos \omega t, \end{aligned} \quad (1)$$

where

$$\begin{aligned} \varepsilon_{\mathbf{k}} = & \{ [2K'S + 2JS(ak)^2] [4\pi\gamma_s M_s + 2JS(ak)^2] \}^{1/2}, \\ S_j^+ = & S^{1/2} \left(\frac{a}{\delta} \right)^{1/2} N^{-1/2} \sum_{\mathbf{k}} e^{-i\mathbf{k}\mathbf{R}_j} \sin \theta_j (u_{\mathbf{k}} a_{\mathbf{k}}^+ + v_{\mathbf{k}} a_{-\mathbf{k}}), \\ S_j^- = & S^{1/2} \left(\frac{a}{\delta} \right)^{1/2} N^{-1/2} \sum_{\mathbf{k}} e^{i\mathbf{k}\mathbf{R}_j} \sin \theta_j (u_{\mathbf{k}} a_{\mathbf{k}} + v_{\mathbf{k}} a_{-\mathbf{k}}^+), \\ S_j^z = & S - S_j^+ S_j^- / 2S, \\ u_{\mathbf{k}} = & 2^{-1/2} \left\{ \frac{2JS(ak)^2 + 2\pi\gamma_s M_s + K'S}{\varepsilon_{\mathbf{k}}} \pm 1 \right\}^{1/2}, \\ v_{\mathbf{k}} = & 2^{-1/2} \left\{ \frac{2JS(ak)^2 + 2\pi\gamma_s M_s + K'S}{\varepsilon_{\mathbf{k}}} \mp 1 \right\}^{1/2}, \end{aligned}$$

J is the exchange interaction constant, N is the total number of spins, M_s is the equilibrium magnetization per unit volume, a is the lattice constant, φ is the angle between the direction of the rf field and the z axis, $\omega_1 = \gamma_s h_1$ is the amplitude of the rf field in units of frequency γ_s is the gyromagnetic ratio, \mathbf{k} is a two-dimensional vector lying in the plane of the wall, and K' is the anisotropy constant corresponding to the quasielastic energy of the wall.

We shall now go over in Eq. (1) to the interaction representation with the Hamiltonian

$$\mathcal{H}_0 = \sum_{\mathbf{k}} \varepsilon_{\mathbf{k}} a_{\mathbf{k}}^+ a_{\mathbf{k}} + \sum_j A \langle S_j^z \rangle I_j^z, \quad (2)$$

where

$$\langle S_j^z \rangle = S - \frac{1}{2} \left(\frac{a}{\delta} \right) N^{-1/2} \sin^2 \theta_j \sum_{\mathbf{k}} \{ v_{\mathbf{k}}^2 + (u_{\mathbf{k}}^2 + v_{\mathbf{k}}^2) \langle n_{\mathbf{k}} \rangle \}$$

$\langle n_{\mathbf{k}} \rangle$ is the average temperature.

The time-dependent Hamiltonian is

$$\begin{aligned} \mathcal{H}(t) = & \sum_{j, \mathbf{k}} \frac{A}{2} \left\{ I_j^- (S)^{1/2} \left(\frac{a}{\delta} \right)^{1/2} N^{-1/2} e^{i\mathbf{k}\mathbf{R}_j} \sin \theta_j \right. \\ & \times (u_{\mathbf{k}} a_{\mathbf{k}}^+ e^{i(\omega_{\mathbf{k}} - \omega_n)t} + v_{\mathbf{k}} a_{-\mathbf{k}} e^{-i(\omega_{\mathbf{k}} + \omega_n)t}) + \text{H.c.} \left. \right\} \\ & + \sum_{\mathbf{k}} \frac{\pi}{2} \sin \varphi \omega_1 (e^{i\omega t} + e^{-i\omega t}) [(u_{\mathbf{k}}^2 + v_{\mathbf{k}}^2) a_{\mathbf{k}}^+ a_{\mathbf{k}} \\ & + u_{\mathbf{k}} v_{\mathbf{k}} (a_{\mathbf{k}}^+ a_{-\mathbf{k}}^+ e^{i2\omega_{\mathbf{k}} t} + a_{\mathbf{k}} a_{-\mathbf{k}} e^{-i2\omega_{\mathbf{k}} t})] \\ & + 2S^{1/2} \left(\frac{\delta}{a} \right)^{1/2} N^{1/2} \cos \varphi (u_0 + v_0) (a_0^+ e^{i\omega_0 t} + a_0 e^{-i\omega_0 t}), \end{aligned} \quad (3)$$

where H.c. denotes the Hermitian conjugate terms: $\omega_{nj} = A \langle S_j^z \rangle$.

Equation (3) is simplified by dropping the terms proportional to I_j^z and the terms which do not contain magnon operators, because they do not contribute to the resonance processes of interest to us. We can conveniently calculate the probabilities of many-quanta resonances using the formalism of the effective Hamiltonian developed in Refs. 11 and 12. To fourth order, the effective Hamiltonian is

$$\begin{aligned} \mathcal{H}_{eff} = & \overline{\mathcal{H}} + \frac{1}{2} [\langle \overline{\mathcal{H}} \rangle, \overline{\mathcal{H}}] + \frac{1}{3} [\langle \overline{\mathcal{H}} \rangle, [\langle \overline{\mathcal{H}} \rangle, \overline{\mathcal{H}} + \frac{1}{2} \overline{\mathcal{H}}]] \\ & + \frac{1}{6} [\langle \overline{\mathcal{H}} \rangle, [\langle \overline{\mathcal{H}} \rangle, [\langle \overline{\mathcal{H}} \rangle, \overline{\mathcal{H}} + \frac{1}{2} \overline{\mathcal{H}}]]] \\ & + \frac{1}{8} [\langle [\langle \overline{\mathcal{H}} \rangle, \overline{\mathcal{H}} + \overline{\mathcal{H}}] \rangle, [\langle \overline{\mathcal{H}} \rangle, \overline{\mathcal{H}} + \overline{\mathcal{H}}]], \end{aligned} \quad (4)$$

where

$$\overline{\mathcal{H}} = \lim_{T \rightarrow \infty} \frac{1}{T} \int_0^T dt \mathcal{H}(t), \quad (5)$$

$$\langle \overline{\mathcal{H}} \rangle = i \int dt' [\mathcal{H}(t') - \overline{\mathcal{H}}], \quad (6)$$

and the average operation in Eq. (5) is applied only to the fast variables, i.e., to the variables for which the oscillation frequency is much higher than the "magnitude" of the Hamiltonian expressed in frequency units.

Substituting Eq. (3) in Eq. (4), we find in the second order that the Hamiltonian describing a one-quantum resonance process is

$$\mathcal{H}^{(1)} = \sum_j \omega_{1j} \cos \varphi \eta_j^{(1)} I_j^+ e^{i(\omega_{nj} - \omega)t} + \text{H.c.}, \quad (7)$$

where

$$\eta_j^{(1)} = \pi A S \gamma_s M_s \sin \theta_j / \gamma_1 \varepsilon_0 \Delta_j, \quad \Delta_j = \omega_{nj} - \omega_0, \quad \omega_{1j} = \gamma_1 h_1. \quad (8)$$

In the derivation of this expression it is assumed that $|\Delta_j| \ll \omega_0, \omega_{nj}$, which is well satisfied in the case of manganese ferrite. Equation (8) is the usual enhancement of the rf field in domain walls. Substituting in Eq. (8) the numerical values of the parameters for MnFe_2O_4 taken from Ref. 13 ($M_s \approx 500$ Oe, $\omega_n \approx 600$ MHz, $\Delta = 100$ MHz, $\lambda_s \approx 2 \times 10^{-20}$ erg/G, $\gamma_1 \approx 2 \times 10^{-23}$ erg/G), we obtain the following order-of-magnitude estimate:

$$\eta_j^{(1)} \sim 10^4.$$

We can similarly obtain expressions for the effective Hamiltonians describing two- and three-quantum resonance processes at frequencies $\omega \sim \omega_n/2$ and $\omega \sim \omega_n/3$:

$$\mathcal{H}^{(2)} = \sum_j \omega_{11} \sin \varphi \cos \varphi \eta_j^{(2)} I_j^+ e^{i(\omega_n/2 - \omega)t} + \text{H.c.}, \quad (9)$$

$$\eta_j^{(2)} = \frac{2\pi AS \gamma_s}{\gamma_I \Delta_j \omega_{nj}} \left(\frac{\pi \gamma_s M_s}{\epsilon_0} \right)^2 \sin \theta_j, \quad (10)$$

$$\mathcal{H}^{(3)} = \sum_j \omega_{11} \sin^2 \varphi \cos \varphi \eta_j^{(3)} I_j^+ e^{i(\omega_n/3 - \omega)t} + \text{H.c.}, \quad (11)$$

$$\eta_j^{(3)} = \frac{45\pi^2 AS \omega_{1s}^2 \gamma_s}{8 \Delta_j \omega_{nj}^2 \gamma_I} \left(\frac{\pi \gamma_s M_s}{\epsilon_0} \right)^3 \sin \theta_j. \quad (12)$$

Numerical estimates of the quantities in Eqs. (11) and (12) give

$$\eta_j^{(2)} \sim 10^3, \quad \eta_j^{(3)} \sim 10^2.$$

Expressions (7), (9), and (11) contain the same factor $\sin \theta_j$. Hence, it follows that the echo spectrum for subharmonics should be identical with the echo spectrum at the fundamental frequency. In the case of $f/2$ this is well supported by the experimental results (see Fig. 3).

Since the pass band of our detector was ~ 1 MHz and the line width for the NMR in a domain wall was ~ 10 MHz, we can assume that the echo is entirely due to a narrow band of spins in the domain wall. If we assume that the echo is due to the Hahn mechanism and that the angles of rotation of the magnetization under the action of the pulses are small ($\ll \pi$), the amplitude of the echo signal is proportional to^{14,15}

$$V \sim \sin A\tau_1 \sin^2(A\tau_2/2),$$

where A is the amplitude of the effective rf field described by Eqs. (7)–(11), and τ_1 and τ_2 are the durations of the first and second pulses.

In the case of small angles of inclination, we have $A\tau_1 \ll 1$ and the dependence of V on τ_1 is linear, in good agreement with the experimental data on one- and two-quantum processes.

CONCLUSIONS

We were able to demonstrate experimentally that the echo signals excited at subharmonic frequencies in MnFe_2O_4 held at $T = 77$ K are due to the ^{55}Mn nuclei located in domain walls and the mechanism responsible for the observed echo signals is that proposed by Hahn. The proposed theoretical model allows for the specific properties of internal wall excitations and the predictions of this model are in qualitative agreement with the experimental data. An improvement in the experimental method should make it possi-

ble to obtain fuller experimental information on the echo at the third subharmonic and to carry out a more detailed comparison of the theory and experiment.

Bearing in mind the results obtained in the present study and those reported in Ref. 16, we may assume that the excitation of echo signals in thin cobalt films¹ is due to a mechanism similar to that proposed in the present study, whereas the echo signals exhibited by lithium ferrite¹ are due to the magnetoelastic effects.

It is of considerable interest to study the properties of subharmonic echo signals at low temperatures because of the possible dynamic frequency shift of the nuclei located in domain walls. The use of manganese ferrite makes it possible to extend the frequency range of the controlled delay of a signal with frequency multiplication (with transformation to the NMR frequency).¹

We can expect that investigations of the properties of the subharmonic echo will make it possible not only to identify directly the spectrum of the nuclei located in domain walls, but also to find the parameters of these walls in magnetically ordered crystals.

The authors are deeply grateful to Yu. M. Bun'kov and V. P. Chekmarev for their great help in preparing the apparatus, and to A. V. Kunevich for supplying the samples.

¹V. I. Dudkin, V. Yu. Petrun'kin, and V. I. Tarkhanov, *Pis'ma Zh. Eksp. Teor. Fiz.* **31**, 330 (1980) [*JETP Lett.* **31**, 301 (1980)].

²A. V. Ivanov, V. R. Korneev, and A. P. Paugurt, *Fiz. Tverd. Tela* (Leningrad) **24**, 883 (1982) [*Sov. Phys. Solid State* **24**, 499 (1982)].

³A. S. Borovik-Romanov, Yu. M. Bun'kov, B. S. Dumesh, M. I. Kurkin, M. P. Petrov and V. P. Chekmarev, *Usp. Fiz. Nauk* **142**, 537 (1984) [*Sov. Phys. Usp.* **27**, 235 (1984)].

⁴Yu. M. Bun'kov and V. V. Dmitriev, *Zh. Eksp. Teor. Fiz.* **80**, 2363 (1981) [*Sov. Phys. JETP* **53**, 1237 (1981)].

⁵V. P. Chekmarev, M. P. Petrov, A. A. Petrov, and V. V. Kulikov, *Pis'ma Zh. Eksp. Teor. Fiz.* **25**, 181 (1977) [*JETP Lett.* **25**, 165 (1977)].

⁶V. P. Chekmarev, V. I. Belotitskiĭ, and G. I. Mamniashvili, *Fiz. Tverd. Tela* (Leningrad) **24**, 222 (1982) [*Sov. Phys. Solid State* **24**, 123 (1982)].

⁷G. I. Mamniashvili and V. P. Chekmarev, *Soobshch. Akad. Nauk Gruz. SSR* **100**, 573 (1980).

⁸E. L. Hahn, *Phys. Rev.* **80**, 580 (1950).

⁹E. A. Turov and M. P. Petrov, *Yadernyy magnitnyĭ rezonans v ferro- i antiferromagnetikakh*, Nauka, M., 1969 (*Nuclear Magnetic Resonance in Ferro- and Antiferromagnets*, Wiley, New York, 1972).

¹⁰J. M. Winter, *Phys. Rev.* **124**, 452 (1961).

¹¹L. L. Buishvili and M. G. Menabde, *V sb.: Radiospektroskopiya* (in: *RF Spectroscopy*), Perm, 1983, p. 3.

¹²L. L. Buishvili, G. V. Kobakhidze, and M. G. Menabde, *Zh. Eksp. Teor. Fiz.* **84**, 138 (1983) [*Sov. Phys. JETP* **57**, 80 (1983)].

¹³S. Krupička, *Physik der Ferrite und der verwandten magnetischen Oxide*, Vieweg, Brunswick, 1973 (Russ. Transl., Mir, M., 1976).

¹⁴A. L. Bloom, *Phys. Rev.* **98**, 1105 (1955).

¹⁵M. I. Kurkin and S. V. Ivanov, *Vozmozhnosti primeneniya metodov YaMR pri izuchenii magnitnoi struktury domennykh grantis* (Potential Applications of NMR Methods in Studies of Magnetic Structure of Domain Walls), Preprint, Institute of Physics of Metals, Ural Scientific Center of the Academy of Sciences of the USSR, Sverdlovsk, 1984.

¹⁶M. Rubinstein and G. H. Stauss, *J. Appl. Phys.* **39**, 81 (1968).

Translated by A. Tybulewicz